International Journal of Heat and Mass Transfer 52 (2009) 2759–2768

Contents lists available at ScienceDirect

International Journal of Heat and Mass Transfer

journal homepage: www.elsevier.com/locate/ijhmt

Heat transfer in evaporating black liquor falling film

M. Johansson [a,*], L. Vamling [a], L. Olausson [b]

[a] Heat and Power Technology, Department of Energy and Environment, Chalmers University of Technology, SE-412 96 Göteborg, Sweden
[b] Metso Power AB, Box 8734, SE-402 75 Göteborg, Sweden

ARTICLE INFO

Article history:
Received 21 February 2008
Received in revised form 14 August 2008
Available online 21 February 2009

Keywords:
Black liquor
Falling film
Evaporation
Heat transfer
Turbulence
High Pr number

ABSTRACT

Black liquor is a fluid with high viscosity, implying high Pr numbers. Most of the previously developed correlations for falling film evaporation heat transfer were developed for fluids with relatively low Pr numbers, and therefore are not valid for most black liquor evaporation conditions. Experimental heat transfer data from black liquor evaporation are presented here. They show that the Nu number, as expected, increases in the turbulent region. However, at a specific Re number for each Pr number level, the Nu number ceases to increase with increasing Re number. A new correlation, taking this observation into account, has been developed on the basis of experimental data in the region of $4.7 < Pr < 170$ and $47 < Re < 6740$, and is presented in this paper. A dry solid content dependence is included in the new correlation and improves its predictions for black liquor.

1. Introduction

In the pulp and paper industry, the black liquor evaporation process is a large energy consumer. About one-third of the steam consumption in an average Swedish non-integrated market kraft pulp mill is consumed by the evaporation plant [1]. The total fuel consumption in the Swedish pulp and paper industry was 55.2 TWh in 2005 [2], which mean that large energy flows are involved in the black liquor evaporation plant. Black liquor is generated during the production of chemical pulp from wood or annual plants; its main constituents are dissolved wood (lignin), cooking chemicals and a large amount of process water.

Research on the energy use in the pulp and paper process has shown that thermal integration of the evaporation with other parts of the process could considerably increase energy recovery and thus save significant amounts of primary steam [3]. The greatest potential for reduction can be achieved in the evaporation plant by combining measures, such as using both medium-pressure steam (10–12 bar (a)) and low-grade process waste heat to drive the evaporator train, and decreasing the lowest condensation temperature. For these measures to be implemented, the gains from the live steam savings should be higher than the increased investment costs that may occur. To get a more reliable basis for judging whether this is the case, increased knowledge about the heat transfer in falling film evaporation of black liquor is essential. The knowledge gives information about how to design energy-optimized evaporation plants where thermal integration can be implemented. Hence this knowledge yields opportunities for cost-effective energy savings and reduced CO_2 emissions.

Previously developed correlations for heat transfer in falling film evaporation were developed for fluids with relatively low Pr numbers. Black liquor is a fluid with high viscosity, especially at high dry solid content or low temperature, which means high Pr numbers.

In earlier work [4], many of the previously developed general correlations for heat transfer in falling film evaporation were compared with experimental heat transfer data for black liquor evaporation. It was concluded that none of the previously developed correlations fit well with the experimental data. However, for Pr numbers above 50, extrapolation of correlations by Chun and Seban [5] and Schnabel and Schlünder [6] lead to values that are closest to the sparse experimental results.

Here an extended set of experimental data is presented. Based on the experimental data for falling film evaporation of black liquor, a new correlation similar to the standard form where $Nu = f(Re, Pr)$ was developed for Pr numbers up to 170.

2. Theory

At flow rates of industrial interest, falling liquid films are usually turbulent and characterized by the formation of waves at the film interface. Understanding the effects of the waves is important in predicting the heat transfer coefficients in falling film evaporation.

Lyu and Mudawar [7] studied falling film flow and found that each large wave in the falling film was followed by a thin film.

* Corresponding author. Tel.: +46 31 7723012; fax: +46 31 821928.
E-mail address: miriam.johansson@chalmers.se (M. Johansson).

0017-9310/$ - see front matter © 2009 Elsevier Ltd. All rights reserved.
doi:10.1016/j.ijheatmasstransfer.2008.09.040

Nomenclature

δ_{Cu}	distance between thermocouples in copper block and tube wall (m)
δ_{film}	falling film thickness (m)
$\delta_{TC,i}$	apparent distance between inside thermocouples in tube wall and inside surface of tube wall (m)
$\delta_{TC,o}$	apparent distance between outside thermocouples in tube wall and outside surface of tube wall (m)
$\delta_{TC,w,l}$	local apparent radial distance between the thermocouples in tube wall (m)
$\delta_{w,l}$	local tube wall thickness (m)
$\delta_{w,l,o}$	apparent distance between thermocouples measuring temperature on the inside of the tube wall and the inside tube wall surface (m)
g	gravitational acceleration (m/s^2)
K	parameter (–)
$P1$	parameter (–)
$P2$	parameter (–)
P_S	parameter (–)
h	heat transfer coefficient (W/m^2 K)
k_{bl}	conductivity of black liquor (W/mK)
k_{Cu}	conductivity of copper block (W/mK)
k_w	conductivity of tube wall (W/mK)
μ	dynamic viscosity (Pa s)
ν	kinematic viscosity (m^2/s)
ρ	density (kg/m^3)
ρ_v	density of vapour (kg/m^3)
σ	surface tension (N/m)
Γ	mass flow rate per unit width (kg/ms)
τ	shear stress (kg/ms^2)
τ_w	wall shear stress (kg/ms^2)
$\dot{\gamma}$	shear rate (1/s)
c_p	specific heat of black liquor (J/kg K)
$c_{p,E}$	excess heat capacity (J/kg K)
c_{p,H_2O}	heat capacity for water (J/kg K)
$c_{p,S}$	heat capacity for solids (J/kg K)
DS	dry solid content (%)
$h_{bl,l}$	local heat transfer coefficient for black liquor film (W/m^2 K)
$h_{c,l}$	local heat transfer coefficient for condensate film (W/m^2 K)
L_{TC34}	apparent distance between thermocouple 34 and tube wall surface (mm)
L_{TC36}	apparent distance between thermocouple 36 and tube wall surface (mm)
k_w	conductivity of tube wall (W/mK)
q_{Cu}	local heat flux over copper block (W/m^2)
q_l	local heat flux over tube wall (W/m^2)
S	dry solid content (weight fraction)
T_{bl}	mixed cup temperature of black liquor falling film (K) or (°C)
$T_{bl,s}$	temperature of black liquor film interface (K)
T_{Cu}	temperature measured by thermocouple in copper block (K)
$T_{Cu,w}$	temperature on tube wall calculated from temperature in copper block (K)
$T_{TC,i,l}$	local temperature measured with TC on inside of tube wall (K)
$T_{TC,o,l}$	local temperature measured with TC on outside of tube wall (K)
$T_{i,l}$	local temperature on inside of tube wall (K)
$T_{o,l}$	local temperature on outside of tube wall (K)
T_s	temperature of saturated primary steam (K)
ΔT_{Cu}	temperature difference in copper block (K)
$\Delta T_{bl,f,l}$	local temperature difference over black liquor film (K)
$\Delta T_{c,f,l}$	local temperature difference over condensate film (K)
$\Delta T_{TC,w,l}$	local temperature difference between thermocouples in tube wall (K)
y	space coordinate perpendicular to the free surface (–)
Ka	Kapitza number $\equiv \frac{\mu^4 g}{\rho\sigma^3}$ (–)
Nu	Nusselt number $\equiv \frac{h}{k}\left(\frac{\nu^2}{g}\right)^{1/3}$ (–)
Pr	Prandtl number $\equiv \frac{c_p\mu}{k}$ (–)
Re	Reynolds number $\equiv \frac{4\Gamma}{\mu}$ (–)

Subscripts

exp	experimental
lam	laminar
limit	limit in the turbulent flow regime where heat transfer does not increase more for increased Γ
TC	thermocouple
trans	transition to turbulent flow regime
turb	turbulent

Mudawar and Houpt [8] found that the temperature profile in the falling film was steep in the thinner parts of the film and in the near-wall region beneath the large wave. But it was fairly flat within the wave itself. This suggests that the liquid in the large waves behaves as an isolated lump undergoing recirculation, instead of continually mixing with the thinner part of the film.

Experimental investigations by Mudawar and Houpt [8] of the falling film reveals that the substrate thickness increases with increasing Prandtl (Pr) number for constant Reynolds (Re) number. The radial velocity component was measured in the falling film for two different experiments with high Pr number, and its magnitude was small in both cases. Examination of the falling film indicated that the large waves at high Pr numbers behaved like lumps of liquid sliding over the substrate. These observations are consistent with those of Lyu and Mudawar [7] who found temperature profiles within large waves to be flat. That is, the fluid within a wave behaved as an isolated lump containing a region of recirculation.

3. Experimental apparatus and procedure

A research evaporator (a pilot plant), built in cooperation with Metso Power AB (previously Kvaerner Power AB), Göteborg, Sweden, was used to study the heat transfer behaviour of falling black liquor films. The heart of the plant is a vertical tube 4.5 m long, with a falling film of black liquor flowing on the outside. The outer diameter of this evaporator tube is 60 mm. Heating is accomplished by condensing steam on the inside of the tube.

The heating steam is distributed along the inside of the evaporator tube, through an internal steam tube. The steam condenses on the inside of the evaporator tube and the condensate forms a falling film. Upstream of the steam tube is a specially designed vessel to ensure saturated steam conditions; see Fig. 1.

With the research evaporator, experiments presented in this paper were performed by running the process at a constant dry solid content, which was maintained by recirculating the secondary condensate from the condenser to the processed black liquor. To

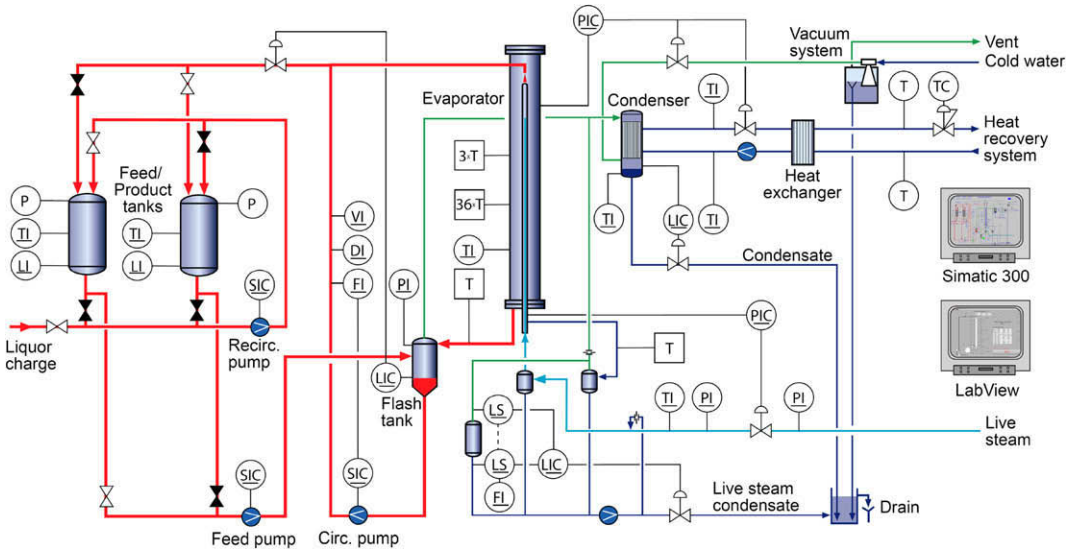

Fig. 1. Flow sheet of the research evaporation plant (the pilot plant).

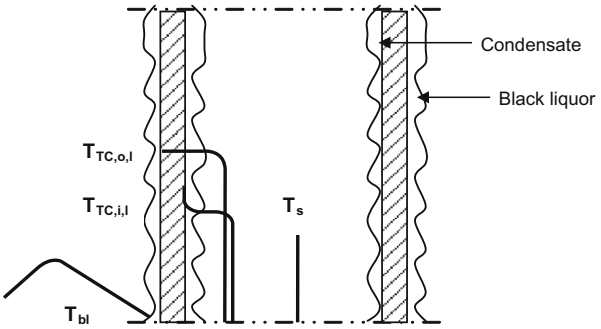

Fig. 2. Thermocouples are mounted to measure the temperature on the inside and outside of the tube wall and in the primary steam, as well as the black liquor mixed cup temperature.

increase the dry solid content of the black liquor between experiments, the secondary condensate was extracted after the condenser.

3.1. Heat flux and heat transfer measurements

To measure heat flux locally, the evaporator tube is equipped with 18 pairs of type K thermocouples mounted at different positions both vertically and circumferentially; see Figs. 2 and 3. The local heat flux of the tube wall, q_l, was obtained as:

$$q_l = \frac{k_w}{\delta_{TC,w,l}} \Delta T_{TC,w,l} \tag{1}$$

where

$$\Delta T_{TC,w,l} = T_{TC,i,l} - T_{TC,o,l} \tag{2}$$

Here k_w is the conductivity of the tube wall, which was calculated from the temperature of the tube wall, and $\delta_{TC,w,l}$ was the local distance between the thermocouples (different for each pair of thermocouples).

The temperature on the outside of the tube wall was calculated from the temperature difference over the wall and the absolute temperature in it, which means that the total temperature

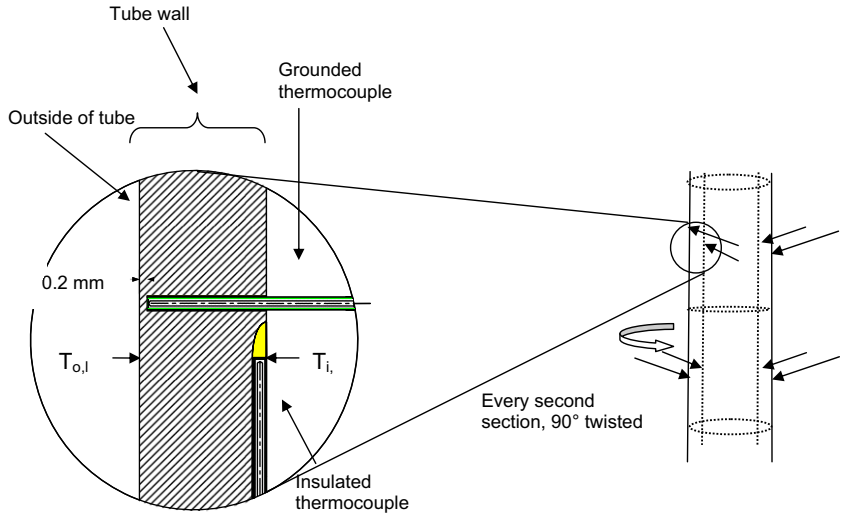

Fig. 3. Thermocouples connected to tube wall. Both thermocouples were connected from the inside of the tube. The vertical thermocouple had an insulated measuring point while the horizontal thermocouple had a grounded measuring point. Each arrow on the tube to the right in the figure indicates one thermocouple. Thermocouple locations are twisted 90° from each other at each height, as the twisted arrow indicates. The temperature was measured at nine different heights.

difference over the tube wall was also calculated. From the inside and outside tube wall temperatures and the local heat flux, the local heat transfer coefficients, for both the condensate film and the black liquor film, were calculated as follows (see also Figs. 2 and 3):

$$h_{bl,l} = \frac{q_l}{\Delta T_{bl,f,l}} \tag{3}$$

and

$$h_{c,l} = \frac{q_l}{\Delta T_{c,f,l}} \tag{4}$$

where

$$\Delta T_{bl,f,l} = T_{o,l} - T_{bl,s} \tag{5}$$

and

$$\Delta T_{c,f,l} = T_s - T_{i,l} \tag{6}$$

where

$$T_{i,l} = T_{TC,i,l} + \frac{(T_{TC,i,l} - T_{TC,o,l})}{\delta_{TC,w,l}} \delta_{TC,i} \tag{7}$$

and

$$T_{o,l} = T_{TC,o,l} - \frac{(T_{TC,i,l} - T_{TC,o,l})}{\delta_{TC,w,l}} \delta_{TC,o} \tag{8}$$

where T_s was the temperature of saturated primary steam, which was the same as the temperature on the condensate film surface. $T_{TC,o,l}$ and $T_{TC,i,l}$ were the local temperatures close to the outside and inside of the tube wall, measured with the thermocouples mounted into the wall. $T_{bl,s}$ was the black liquor film interface temperature, which was calculated from measurements with a thermocouple mounted into a cup in the bottom of the evaporator, where the black liquor film falls down before it leaves the evaporator.

The tube wall thickness was 5 mm, greater than that commonly used in industry, and was selected in order to improve the accuracy of the heat flux measurement. To further improve the accuracy, thermocouples with a grounded measuring point were used at the outer wall, since this kind of sheeting makes it possible to determine the location of the measuring point with higher accuracy and thus the distance between the thermocouples.

To reduce the risk of disturbing the falling film flow pattern and the risk of corrosion, the outer surface thermocouple was soldered into a hole that was drilled from the inside of the evaporator tube and almost to the outside of the tube. Only 0.2 mm of the tube wall was left (see Fig. 3). For the thermocouples measuring the temperature on the inside of the tube, the notches were made 1.1 mm deep.

The temperature was measured at nine different heights on the evaporator tube, where level 1 was the level closest to the outlet and level 9 was the level closest to the top. There was 0.5 m between each level and the next.

3.2. Thermocouple position calibration

Despite careful individual, as well as pair-wise, calibration of thermocouples before assembly, preliminary experiments showed unexpected deviations between the heat transfer coefficients measured with different pairs of thermocouples, i.e. at different positions along and around the tube. The differences in temperature for local measurements at different locations along the tube wall were about ±0.6 °C. The reason for the large deviations in the local temperature measurements was investigated. Experimental details are given by Johansson et al. [9].

3.2.1. Analysis with X-ray microscopy

One part of the investigation was to analyse the thermocouple soldering. An analysis with X-ray microscopy with high-voltage supply was done with seven thermocouples that were soldered into holes in the tube material (Duplex SAF 2205), using exactly the same procedure as when mounting the thermocouple into the evaporator tube wall. The analysis showed that air was located in the bottom of the hole and up along the thermocouple side at some of the thermocouple solderings.

3.2.2. Finite-element method calculations

The conduction in the solder significantly affects the temperature profiles close to the measuring points. To estimate the size of this influence, a CFD analysis with finite-element-based calculations of the temperature profiles was carried out, using the commercial COMSOL Multiphysics FEMLAB software. With these simulations, the apparent location of the thermocouple measuring point was calculated, for a thermocouple physically mounted into the bottom of the drilled hole. The thermal conductivity of a solder material with similar composition was measured [10] and from this the conductivity of the solder material used was calculated and used in the FEMLAB simulations.

Simulations with the FEMLAB software showed that the area between the thermocouple tip and the bottom of the drilled hole was important for the temperature measurements. There was a significant difference in what temperature the thermocouple measured, depending on whether this area was filled with air or with the solder material. The apparent position was found to be 0.65–2.25 mm from the outside tube wall depending on how much of the drilled hole was filled with solder material. This should be noted as another important parameter.

3.2.3. Thermocouple average apparent position

The problem of a deviating local heat transfer coefficient was initially handled by calibrating the average heat transfer coefficient. This calibration was done with experiments with evaporating water. The parameter that was set by the calibration was the average apparent position of the thermocouples mounted into the tube wall. The experimental heat transfer results were compared with results from the heat transfer correlation developed by Schnabel and Schlünder [6] which is a commonly used correlation, valid for water. In this comparison it was found that an average apparent position of 1.2 mm from the outside of the wall for the thermocouple measuring the temperature on the outside of the wall, and an average apparent position of 0.6 mm from the inside of the wall for the thermocouple measuring the temperature on the inside of the wall, agreed with the correlation by Schnabel and Schlünder [6].

3.2.4. Calibration of the apparent positions of TC 34 and TC 36

A calibration of the apparent positions of thermocouples 34 and 36 was carried out to improve the accuracy of these two local heat flux and heat transfer measurements. Thermocouples 34 and 36 are located close to the sight glasses farthest down on the evaporator, about 4 m from the top of the evaporator tube.

The position calibration was carried out with a construction of thermocouples mounted into blocks of copper. There was one block for each thermocouple that was position-calibrated, which means two blocks with two thermocouples in each block.

The objective was to calculate the apparent positions of thermocouples 34 and 36, which were mounted into the tube wall to measure the temperature on the outside of the tube wall. This was done by calculating the temperature on the tube wall surface with the thermocouples that measured the temperature in the copper block, knowing that the temperature measured by the

thermocouples in the tube wall would be the same if its apparent position was at the tube wall outside surface.

The temperature on the tube wall's outside surface, from the thermocouples in the copper block, was calculated as:

$$T_{Cu,w} = T_{Cu} + \Delta T_{Cu} \tag{9}$$

$$q_{Cu} = \frac{k_{Cu}}{\delta_{Cu}} \Delta T_{Cu} \tag{10}$$

where $\delta_{Cu} = 2.5$ mm and $k_{Cu} = f(T_{Cu})$.

$$q_l = \frac{k_w}{\delta_{TC,w,l}} (T_{TC,i,l} - T_{TC,o,l}) \tag{11}$$

where $\delta_{TC,w,l} = \delta_{w,l} - 0.6 \times 10^{-3} - \delta_{w,l,o}$ and $k_w = f(T_{TC,o,l})$ and $\delta_{w,l,o}$ was the local apparent distance between the outer tube wall and the measuring point, which gave the apparent position of the thermocouple.

$$q_{Cu} = q_l \tag{12}$$

The temperature on the tube wall surface from the thermocouples in the tube wall was calculated as:

$$T_{o,l} = T_{TC,o,l} - \frac{(T_{TC,i,l} - T_{TC,o,l})}{\delta_{TC,w,l}} \delta_{w,l,o} \tag{13}$$

Solving this system of equations and finding $\delta_{w,l,o}$ results in $T_{Cu,w} = T_{o,l}$

$$\rightarrow \delta_{w,l,o} = \frac{k_w \frac{\delta_{Cu}}{k_{Cu}} (T_{TC,i,l} - T_{TC,o,l}) - (\delta_{w,l} - 0.6 \cdot 10^{-3})(T_{TC,o,l} - T_{Cu})}{(T_{Cu} - T_{TC,i,l})} \tag{14}$$

The calculated apparent position was different for the two thermocouples (see Fig. 4).

The knowledge gained about the apparent position of the two thermocouples was used for recalculation of the two local heat transfer coefficients at level 2 in the evaporator. In Fig. 5 are the local heat transfer coefficients for experiments with water.

As was seen in Fig. 5, the local heat transfer coefficients, calculated with the equations for the apparent positions for the thermocouples measuring the temperature on the tube wall outside, are more similar to each other than the local heat transfer coefficient calculated with the average position of the thermocouples. This points to more accurate local heat transfer coefficient calculations.

3.2.5. Estimation of the apparent positions for the other thermocouples

From the position calibration of thermocouples 34 and 36, a position adjustment of the rest of the thermocouples was done. This position adjustment was done by studying some experimental data from evaporation experiments with water. By assuming that all heat transfer coefficients in the falling water film should be equal to the heat transfer coefficient calculated from thermocouples 34 and 36, the apparent position of the rest of the thermocouples measuring the temperature on the outside tube wall was found. Using these position estimates, the average heat flux and heat transfer coefficient were calculated.

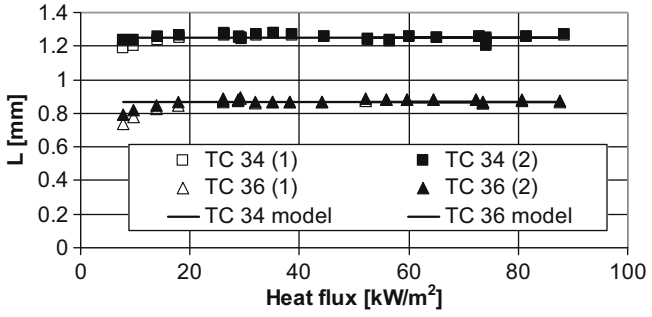

Fig. 4. The experimental data from the position calibration show the apparent position of the measuring points of the two thermocouples. The filled lines are the models developed from the experimental data, where the apparent positions are considered to be constants.

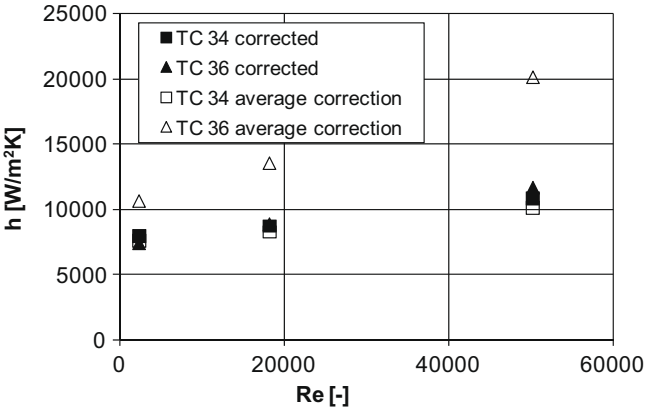

Fig. 5. Experiments where water is evaporated at about 100 °C, with a total temperature difference of about 8 °C. The local heat transfer coefficients at level 2 on the evaporator tube are calculated in two different ways: with the apparent position gained from the position calibration (see Section 3.2.4), and using the average position of the thermocouples (see Section 3.2.3).

3.3. Additional experimental equipment

Additional experimental data obtained from the research evaporation plant are the following:

- Inlet mass flow (and density) of black liquor in the evaporator (from measurement equipment placed in the circulating flow of black liquor to the evaporator).
- Inlet viscosity of black liquor in the evaporator (measurement equipment placed in the circulating flow of black liquor to the evaporator).
- Volume flow of steam condensate (equipment measuring the steam condensate flow from the evaporator).
- Temperatures:
  - Temperature into and out of the evaporator on both steam side and black liquor side.
  - Temperature of secondary steam in the evaporator vessel.
  - Bulk temperature of the black liquor in the bottom of the evaporator.
- Pressure on both heating steam side and black liquor side in the evaporator.

3.3.1. Viscosity measurements

The process viscometer used in this work was a Marimex ViscoScope – Sensor VA-300L. The process viscometer measures the viscosity of liquids continually inline. The viscosity was obtained with the torsional oscillation principle. The viscometer measured the viscosity at a shear rate of 3450 1/s. The process viscometer measured the viscosity of the circulating black liquor going to the top of the evaporator tube.

To find out the rheological behaviour of the black liquor a rheometer was used. The laboratory rheometer used was a Bohlin Instruments Rheometer CS50. In this study, an open system and a high-pressure cell with rotating cylinder were used. The rheometer was equipped with an integrated bath through which the temperature was controlled. The rheometer was validated with standard oil

(96 mPa s at 25 °C). It was found that the error related to the instrument was less than 1% for the open measuring systems and less than 4% for the measuring system with the high-pressure cell.

Measurements with the laboratory rheometer and inline viscometer show that the investigated black liquor was non-Newtonian. The viscosity decreases with increasing shear rate, which resulted in a higher measured viscosity with the laboratory rheometer than with the inline viscometer. To calculate the viscosity in the falling film, the shear rate and shear stress in the falling film were calculated. The wall shear stress was calculated from [11]:

$$\tau_w = \rho \cdot \delta_{\text{film}} \cdot g \tag{15}$$

With no interfacial shear, the shear stress distribution across the film was linear, approximating the tube wall as a plate:

$$\frac{\tau}{\tau_w} = 1 - \frac{y}{\delta} \tag{16}$$

The average value of the shear rate in the falling film was used to estimate the average viscosity in the film. The average shear rate ($\dot{\gamma}$) was calculated from an iterative procedure with the following equation [11]:

$$\frac{\tau_w}{2} = -\mu(\dot{\gamma}) \cdot \dot{\gamma} \tag{17}$$

By studying the viscosity and the shear rate in the experiments, a simplification of the calculation above was made. The viscosity used in the calculation of the Nu number was 1.6 times the viscosity according to the inline viscometer.

The viscosity values used in the calculation were also corrected for the difference in temperature and dry solid content in the inline viscometer and the evaporator, according to a correlation for black liquor viscosity developed by Wennberg [12]. The black liquor cup temperature was used as the temperature at which the viscosity was evaluated. The dry solid content used for the evaluation was the average dry solid content between the inlet and outlet from the evaporator.

Further experimental details are given in references [4,13,14].

3.4. Experimental conditions

During the experiments in the research evaporator, the dry solid content was kept constant by bringing the secondary condensate from the condenser back to the processed black liquor. The pressure on the black liquor side, as well as the steam side, was regulated by control valves to be constant during the experiments.

The conditions in each experiment performed at the research evaporator were kept constant during at least 2 h to collect data. The same black liquor was adopted for experiments under a couple of months. With time, it was seen that the black liquor viscosity decreased for the same conditions in the research evaporator and the same dry solid content of the black liquor. The black liquor became heat-treated during the experiments because of the elevated temperatures and the long exposure time. This effect implies that the viscosity data for a given dry solid content are not indicative of black liquor viscosity with the same dry solid content for normal industrial mills; the viscosity data in the experiments presented here are about 50% lower.

3.5. Calculation procedure

The experimental local heat transfer coefficients were calculated with Eqs. (1)–(8) given in Section 3.1.

To enable use of dimensionless expressions, the Nu, Re and Pr numbers are calculated. For calculation of these dimensionless numbers the properties of the black liquor were calculated or measured. The viscosity and density of the black liquor were measured as described above. The conductivity and heat capacity of the black liquor were calculated with the correlations given below.

Thermal conductivity of black liquor [15]:

$$k_{bl} = 0.00144T_{bl} - 0.335S + 0.58 \tag{18}$$

where T_{bl} is in °C and the dry solid content, S, is a value between 0 and 1. This equation can be used over the range of dry solid contents from 0% to 82% and temperatures from 20 to 100 °C.

The dry solid content of the black liquor was measured from black liquor samples that were taken out of the evaporator, using TAPPI test method T650 om-89. The samples correspond to the black liquor dry solid content at the top of the evaporator tube. The increase in dry solid content over the evaporator tube was calculated, and the average between the inlet and outlet black liquor dry solid contents was used in the calculations.

The heat capacity was calculated from a linear mixing rule for water and black liquor solids that works for estimating the heat capacity of black liquor below 50% dry solid content:

$$c_p = (1 - S)c_{p,w} + S \cdot c_{p,s} + c_{p,E} \tag{19}$$

$$c_{p,s} = 1684 + 4.47T_{bl} \tag{20}$$

$$c_{p,E} = (4930 - 29T_{bl})(1 - S)S^{3.2} \tag{21}$$

where T_{bl} is the temperature in °C and the dry solid content, S, is a value between 0 and 1 [15].

Γ was calculated from the circulation flow measured by the mass flow measurement equipment divided by the wetted perimeter (outside perimeter of tube).

To develop a new correlation from the experimental data, the optimization routine *nlinfit* in the numerical software *Matlab* was used. The routine *nlinfit* is a nonlinear least-squares data fitting by the Gauss–Newton method, which estimates the coefficients of a nonlinear function by using least squares.

3.6. Difference in dry solid content

The difference in dry solid content at the top and bottom of the evaporator tube was between 0.3% and 4.5% in the experiments. The largest differences in dry solid contents were found in experiments with low Γ, while high Γ gave small differences (Fig. 6). The outlet dry solid content affects the evaporating black liquor temperature, which is seen in Fig. 7.

In Fig. 7 the black liquor cup temperature was plotted vs. Γ. Higher outlet dry solid content was achieved at lower mass flow rates, which gave higher black liquor cup temperature because of higher boiling point rise at constant pressure.

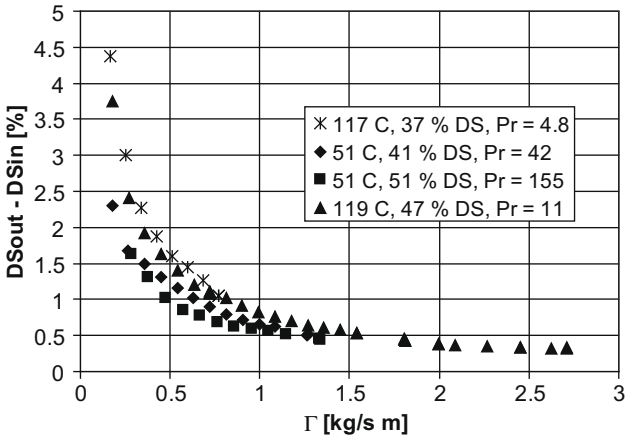

Fig. 6. Difference in dry solid content at top and bottom of the evaporator tube vs. Γ.

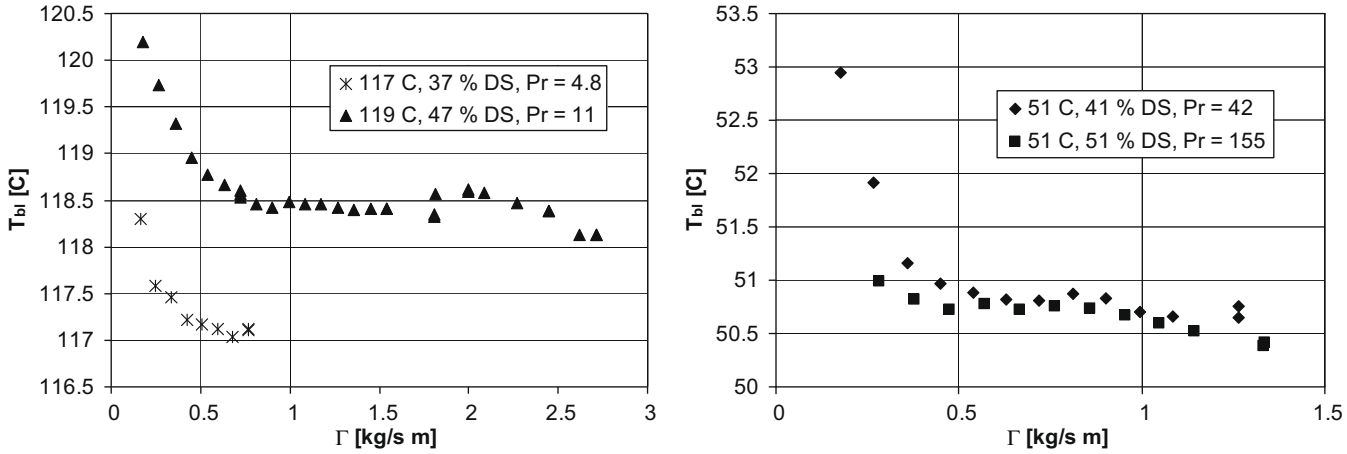

Fig. 7. Black liquor cup temperature vs. Γ.

This means that the dry solid content, and thereby the film interface temperature, at the top of the evaporator tube were lower than in the bottom of the tube, especially for low Γ. This was adjusted for in the calculation of the local heat transfer coefficients.

4. Results with comments

A number of experiments were performed with black liquor. Results presented here are all based on experiments with the same batch of softwood black liquor from a Swedish kraft pulp mill.

4.1. Experimental heat transfer data

The local heat transfer coefficients were calculated with thermocouple positions estimated as described in Section 3.2.5. In the figures presented here, the average heat transfer coefficient is shown. This coefficient was calculated from thermocouple measurements on levels 1–5 (of nine levels, level 1 at bottom) on the evaporator tube, i.e. only values from the fully developed flow were included.

As is seen in Fig. 8, the heat transfer coefficient initially (for low values of Γ) decreases with increasing Γ for most conditions. In this Γ range, the flow had not reached the turbulent flow regime and was still laminar/wavy-laminar. For increased Γ there was a transition to the turbulent flow regime and the heat transfer coefficient increased with Γ, as it should do according to existing general correlations for heat transfer in falling film evaporation for turbulent flow. However, at high Γ, the heat transfer was constant or in some cases even decreased with increasing Γ (See Figs. 8 and 9). There is a limit where the heat transfer coefficient ceases to increase with Γ. Such a limit was not observed in water experiments, nor in the earlier black liquor experiments [4].

4.2. Re number limit for stagnant heat transfer

In Fig. 10 the experimental results were presented using dimensionless numbers. The same trend that was seen in Fig. 8 was also seen in Fig. 10. In the laminar flow regime, with increasing Re number, the Nu number decreases in the laminar flow regime and increases in the turbulent region, which it is expected to do. For a specific Re number at each Pr number level, the Nu number ceases to increase with increasing Re number. The Pr numbers where the limit in Re number occurred were plotted in Fig. 11.

This limit in Re number in these experiments can be described with the following equation:

$$\mathrm{Re}_{\mathrm{limit}} = 13500 \cdot \mathrm{Pr}^{-0.85} \tag{22}$$

Note that the Re number limit for stagnant heat transfer should not be confused with the transitional Re number, which describes at what Re number there is a transition to the turbulent flow regime.

4.3. New correlations

A new heat transfer correlation, using the standard form $\mathrm{Nu} = K \cdot \mathrm{Re}^{P1} \cdot \mathrm{Pr}^{P2}$ for the turbulent part, was developed. Several different versions of correlations were investigated.

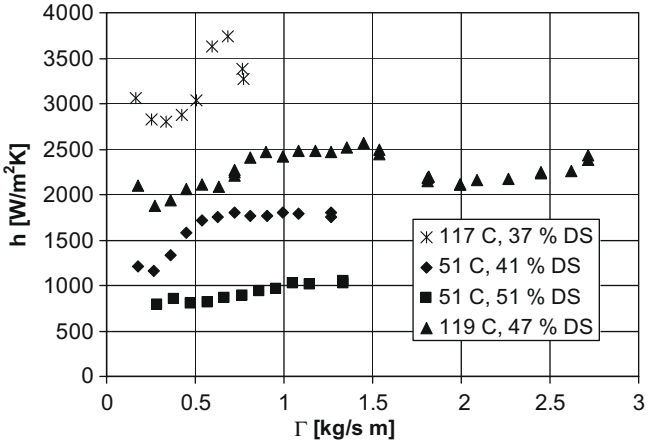

Fig. 8. Heat transfer coefficient (h) vs. circulation flow (Γ).

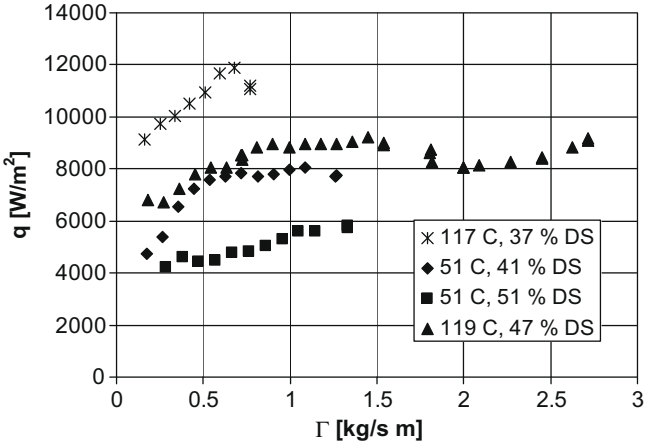

Fig. 9. Transferred heat (q) vs. circulation flow (Γ).

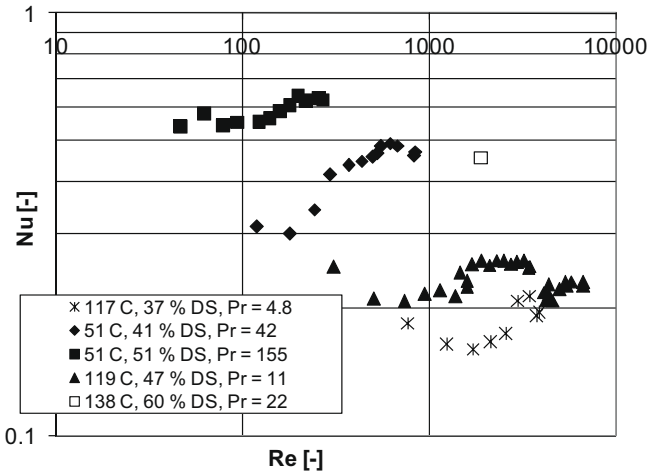

Fig. 10. Experimental Nu number vs. Re number.

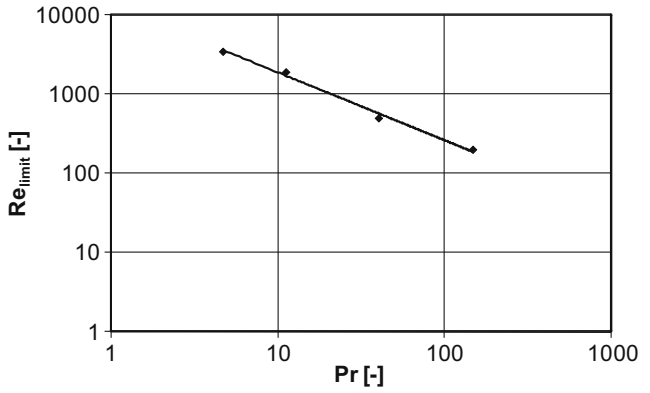

Fig. 11. Limit in Re number where the Nu number ceases to increase with increasing Re number. This Re number is plotted as a function of the Pr number.

By residual analysis it was found that adding a dependence of the dry solid content improved the fit significantly. We found that the best way to add a dry solid content parameter was on the Re number exponent P_s. Concerning the other parameters in the correlation, it was found that the parameters suggested by Schnabel and Schlünder [6] mostly were within the confidence interval of these parameters. Therefore, the correlation developed by Schnabel and Schlünder [6] became the basis for the new correlation. Adding the dry solid content dependence, and including the Re number limit for increase in Nu number described by Eq. (22), the model becomes:

$$\mathrm{Nu}_{\mathrm{lam}} = 1.43 \cdot \mathrm{Re}^{-1/3} \tag{23}$$

$$\mathrm{Nu}_{\mathrm{turb}} = 3.6 \cdot 10^{-3} \cdot \left[\min\left(\mathrm{Re}_{\mathrm{exp}}, \mathrm{Re}_{\mathrm{limit}}\right)\right]^{(0.4-P_S \cdot S)} \cdot \mathrm{Pr}^{0.65} \tag{24}$$

$$\mathrm{Nu} = \left(\mathrm{Nu}_{\mathrm{lam}}^2 + \mathrm{Nu}_{\mathrm{turb}}^2\right)^{1/2} \tag{25}$$

where $\mathrm{Re}_{\mathrm{limit}}$ is given by Eq. (22), S is the dry solid content (in weight fraction) and P_s is a dry solid content parameter found in Table 1.

Table 1
The confidence interval for the parameter in the new correlation.

Parameter	Parameter value and confidence interval
P_s	0.125 ± 0.013

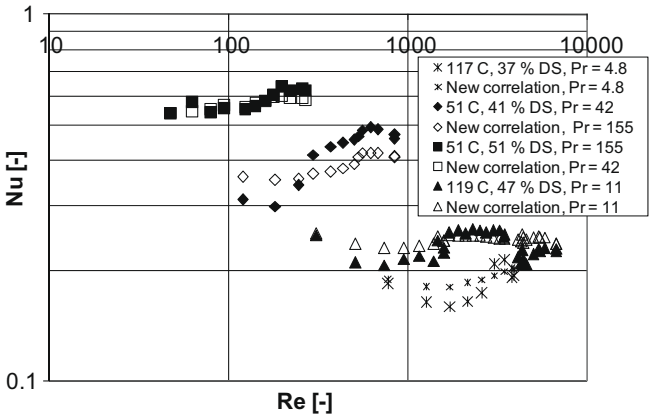

Fig. 12. Nu number vs. Re number, experimental values compared with the new correlation presented in this paper including the limit in heat transfer at higher Re numbers.

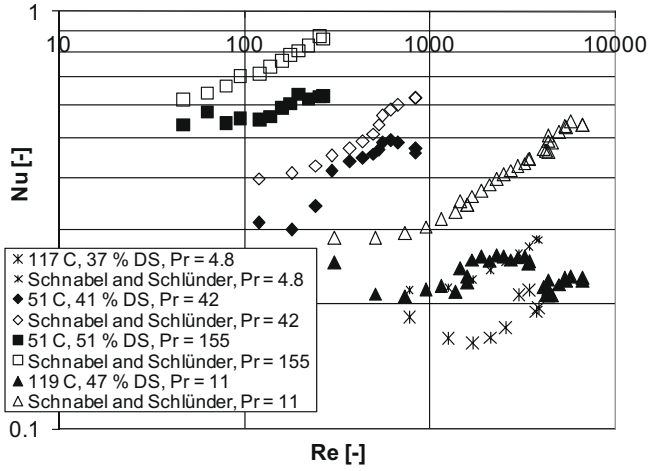

Fig. 13. Nu number vs. Re number, experimental values compared with the correlation developed by Schnabel and Schlünder [6].

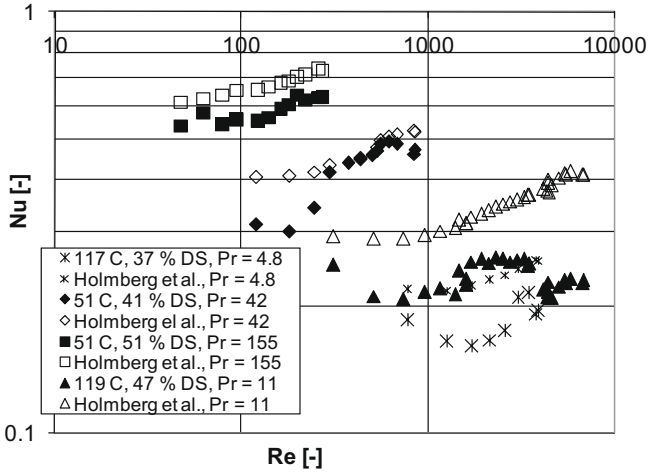

Fig. 14. Nu number vs. Re number, experimental values compared with the correlation developed by Holmberg et al. [19].

The expression $[\min(\mathrm{Re}_{\mathrm{exp}}, \mathrm{Re}_{\mathrm{limit}})]$ in Eq. (24) means that the lowest of $\mathrm{Re}_{\mathrm{exp}}$ and $\mathrm{Re}_{\mathrm{limit}}$ should be used.

Table 2
Transition to turbulent flow regime in the experiments according to Chun and Seban [5] and experimental data.

Experiments	Pr	Re_{trans} (Chun and Seban [5])	Re_{trans} (Schnabel and Schlünder [6])	Re_{trans} (new correlation)	Re_{trans} (experimental data)
117 °C, 37% DS	4.8	1100	872	1297	1721
51 °C, 41% DS	42	110	127	175	181
51 °C, 51% DS	155	28	40	54	
119 °C, 47% DS	11	457	418	661	736

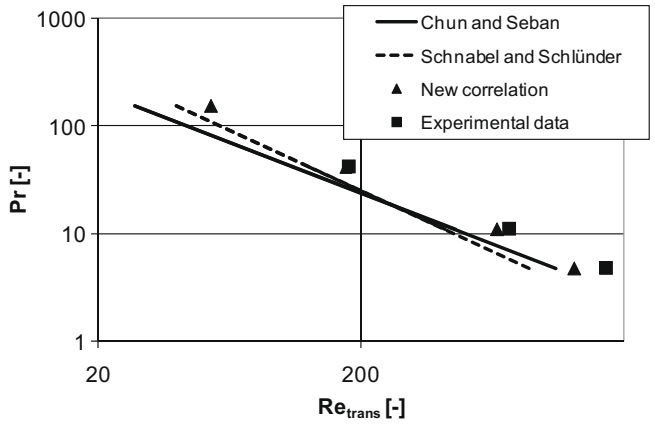

Fig. 15. Transition to turbulent flow regime, Re_{trans}, vs. Pr number according to Chun and Seban [5], Schnabel and Schlünder [6], the new correlation, and the experimental data.

The correlation was developed from experimental data in the region of 4.7 < Pr < 170 and 47 < Re < 6740, and dry solid contents up to 51%. Experiments were also done with a dry solid content of 60%, but there were difficulties in getting a smooth-looking falling film flow at this dry solid content. The falling film flow was rough and disturbed for both lower and higher circulation flows and pressures. The black liquor also started to scale on the evaporator tube after some hours.

This new correlation (Eqs. (22)–(25) and Table 1) was used in Fig. 12, where the correlation was compared with the experimental values.

4.4. Comparison between experimental data and previously developed general correlations

The experimental data from this study were compared with several general correlations from the literature [5,6,16–21], two of which [6,19] are seen in Figs. 13 and 14.

None of the previously developed correlations are in agreement with the experimental data. All of them over-predict the Nu number when compared to the experimental data. Interesting to note is that the correlation developed by Holmberg et al. [19] agrees better with the experimental data at high Pr numbers than at low Pr numbers; see Fig. 14.

4.5. Transition to turbulent flow regime

Regarding at what Re number there is a transition to the turbulent flow regime, Chun and Seban [5] suggest:

$$Re_{trans} = 5800 Pr^{-1.06} \quad (26)$$

This Re_{trans} was found by setting $Nu_{lam} = Nu_{turb}$ in their heat transfer correlation. In Table 2 and Fig. 15 these values are compared with transition values obtained in the same way for the correlation by Schnabel and Schlünder [6] and the new correlation. In the table and the figure are also values obtained from observation of min(Nu) for each Pr number level of the experimental data.

It can be seen in Fig. 15 that the transition to the turbulent flow regime in the experiments performed in this study seems to occur at higher Re numbers than what Chun and Seban [5] and Schnabel and Schlünder [6] suggest. Their correlations are based on data from experiments with fluids with lower Pr numbers. The new correlation agrees better with the observed transition.

5. Discussion

Experiments with an industrial black liquor evaporator have shown that the heat transfer does not increase as much as expected according to general correlations, such as that of Schnabel and Schlünder [6] for heat transfer in falling films with increased circulation flow [22]. However, predicting the increase in heat transfer with the newly developed correlation gives good agreement with the results from the experiments in the industrial evaporator. The reason for the difference between the results from the industrial experiments and those from the correlation of Schnabel and Schlünder [6] could be the latter's lack of two factors in the new correlation: the dry solid content dependence and the limit where the Nu number ceases to increase with increasing Re number.

The dry solid content dependence in the new correlation, which is associated with the turbulent Re number, reduces the effect of increased heat transfer for increased Re number in the turbulent flow regime. There are likely to be significant mass transfer resistances in the black liquor falling film, which probably increase with increased dry solid content. The effect of these resistances in the evaporating film should be further investigated.

Two plausible reasons why the Nu number ceases to increase are discussed here. One is that the liquid in the large waves in the falling film behaves as isolated lumps undergoing recirculation, and the other is sputtering at high circulation flows. The first reason, based on observations by Mudawar and Houpt [8], could explain the heat transfer behaviour of the black liquor with high Pr number. The explanation suggested, from the experimental results and from their observations, was that for increased Γ, larger isolated lumps with internal mixing are created, but there is no increased mixing with the substrate and consequently no increased heat transfer. The increased Γ means increased film thickness, which decreases the effect of liquid–vapour interface evaporation, which lowers the heat transfer coefficient. Increased turbulence (mixing) increases the heat transfer at higher flows, but without this effect the heat transfer coefficient does not continue to increase for increased flow.

Regarding the second reason, the research evaporator was equipped with sight glasses from which the falling film could be studied. The evaporating falling film often looked disturbed, at both higher and lower circulation flow. According to stability theory for the waves, vertical falling film flow is practically always unstable [23]. At lower circulation flows, some bubbles appear at the film surface. At higher flows, bubble bursting produced black liquor drops that left the falling film in a process called sputtering. Due to sputtering, the film progressively gets thinner along the evaporator tube, leading to a decrease in the falling film velocity. Since the heat transfer coefficient depends on the falling film

velocity, lower flow because of sputtering decreases the heat transfer coefficient [24]. The sputtering tendency was higher at low temperature/pressure evaporation conditions.

6. Conclusions

The experimental Nu number for falling film evaporation of black liquor increases, as expected, in the turbulent region. However, at a specific Re number for each Pr number level, the Nu number ceases to increase with increasing Re number. This limit in Re number in these experiments was described with an equation of the form $\mathrm{Re} = f(\mathrm{Pr})$, and explained in terms of the falling film's movements.

A new correlation, using the standard form $\mathrm{Nu} = K \cdot \mathrm{Re}^{P1} \cdot \mathrm{Pr}^{P2}$ for the turbulent part, was developed from the experimental data. A dry solid content dependence parameter was added to the new correlation. This correlation describes the experimental data within ±15%. None of the investigated general correlations from literature was found to be in agreement with the presented experimental data.

Acknowledgments

The authors gratefully acknowledge the Swedish Energy Agency and Metso Power AB for financial support for this work. We kindly thank Mathias Gourdon and Bengt Erichsen (both at the Department of Heat and Power Technology at Chalmers University of Technology) for their valuable contribution to this work. We also thank Jon van Leuven for editing.

References

[1] KAM, Ecocyclic Pulp Mill – "KAM". Final report 1996–2002, KAM report A100, STFI (2003) 215.
[2] SCB, 2008. Available from: <www.scb.se> (2008-01-16).
[3] J. Algehed, T. Berntsson, Evaporation of black liquor and wastewater using medium-pressure steam: simulation and economic evaluation of novel designs, Appl. Therm. Eng. 23 (4) (2003) 481–495.
[4] M. Johansson, L. Vamling, L. Olausson, Falling film evaporation of black liquor – comparison with general heat transfer correlations, Nordic Pulp Paper Res. J. 21 (4) (2006) 496–506.
[5] K.R. Chun, R.A. Seban, Heat transfer to evaporating liquid films, J. Heat Transfer Trans. ASME (1971) 391–397.
[6] G. Schnabel, E.U. Schlünder, Wärmeübergang von senkrechten Wänden an nichtsiedende und siedende Rieselfilme. "Heat transfer from vertical walls to falling liquid films with or without evaporation", Verfahrenstechnik 14 (2) (1980) 79–83.
[7] T.H. Lyu, I. Mudawar, Statistical investigation of the relationship between interfacial waviness and sensible heat transfer to a falling liquid film, Int. J. Heat Mass Transfer 34 (6) (1991) 1451–1464.
[8] I. Mudawar, R.A. Houpt, Measurement of mass and momentum transport in wavy-laminar falling liquid films, Int. J. Heat Mass Transfer 36 (17) (1993) 4151–4162.
[9] M. Johansson, L. Vamling, L. Olausson, Indirect methods to determine apparent position in a falling film heat transfer measurement equipment, Internal report, 2007.
[10] Y.S. Touloukian, Thermophysical properties research center, thermophysical properties of matter: the TPRC data series: a comprehensive compilation of data. 1. Thermal conductivity. Metallic elements and alloys by the Thermophysical properties research center (TPRC), in: Y.S. Touloukian, series ed., C.Y. Ho, series technical ed., Purdue University, New York: diagr., tab., 1970.
[11] R.B. Bird, W.E. Stewart, E.N. Lightfoot, Transport Phenomena, second ed., Wiley, New York, 2002. p. 895.
[12] O. Wennberg, Rheological properties of black liquor, in: Proceedings of International Chemical Recovery Conference Ottawa, Canada, April 3–6, 1989, pp. 89–93.
[13] M. Johansson, Heat transfer in falling film evaporation of black liquor – experiments and theory, Lic. thesis, Chalmers University of Technology, Göteborg, Sweden, 2006.
[14] M. Johansson, L. Olausson, L. Vamling, A new test facility for black liquor evaporation, in: Proceedings of Heat-SET 2005 Conference, Heat Transfer in Components and Systems for Sustainable Energy Technologies France, Grenoble, 4–7 April 2005, pp. 159–164.
[15] T.N. Adams, W.J. Frederick, T.M. Grace, M. Hupa, K. Iisa, A.K. Jones, H. Tran, Kraft Recovery Boilers, Tappi Press, American Forest & Paper Association, New York, 1997. p. 381.
[16] A.A. Alhusseini, K. Tuzla, J.C. Chen, Falling film evaporation of single component liquids, Int. J. Heat Mass Transfer 41 (12) (1998) 1623–1632.
[17] A. Åsblad, T. Berntsson, Surface evaporation of turbulent falling films, Int. J. Heat Mass Transfer 34 (3) (1991) 835–841.
[18] M. Härkönen, A. Aula, A. Aittomaki, Heat transfer and hydrodynamics of falling liquid films, Acta Polytech. Scand., Mech. Eng. Ser. (115) (1994) 2–68.
[19] P.A. Holmberg, T. Berntsson, L. Persson, Heat transfer in a falling film lithiumbromide–water evaporator – an experimental study, in: Proceedings of XVIII International Congress of Refrigeration Montreal, Canada, 10–17 August 1991, p. 1485.
[20] I.A. Mudawwar, M.A. El-Masri, Momentum and heat transfer across freely-falling turbulent liquid films, Int. J. Multiphase Flow 12 (5) (1986) 771–790.
[21] V.V. Wadekar, Heat transfer to falling liquid films with high Prandtl numbers, in: Proceedings of the Third European Thermal Science Conference 2000, 2000.
[22] L. Olausson, Personal communication with Lars Olausson at Metso Power AB, Göteborg, Sweden, 2007.
[23] T. Kunugi, C. Kino, DNS of falling film structure and heat transfer via MARS method, Comput. Struct. 83 (6–7) (2005) 455–462.
[24] M. Johansson, I. Leifer, L. Vamling, L. Olausson, Falling film hydrodynamics of black liquor under evaporative conditions, Int. J. Heat Mass Transfer, accepted for publication.